

# Quarterly Progress Report of the PSI-Center (October – December 2009)

by

*Thomas Jarboe, Alan Glasser, Richard Milroy, Brian Nelson,  
Uri Shumlak, and Carl Sovinec*

The Plasma Science and Innovation Center (PSI-Center) has accomplished a great deal this quarter. The PSI-Center is organized into four groups: Boundary Conditions and Geometry, Two-Fluid and Transport, FLR and Kinetic Effects, and Interfacing. Each group has made good progress and the results from each group are given in detail.

**Progress Report for the BC&G Group** (*U. Shumlak, A. Glasser, W. Lowrie, G. Marklin, and E. Meier*)

## Accomplishments

- Our Computer Physics Communications article is accepted for publication: E.T. Meier, V.S. Lukin, U. Shumlak, Spectral element spatial discretization error in solving highly anisotropic heat conduction equation, *Comp. Phys. Comm.*, 2009 (doi:10.1016/j.cpc.2009.12.018)
- The so-called critical ionization velocity (CIV) effect has been added to the plasma-neutral fluid model in SEL/HiFi. The fluid model cannot capture the mechanism for CIV, which involves energy transfer from neutrals to electrons via instability, so a phenomenological model is used. Simulations of plasma acceleration through neutral gas have demonstrated the capability of capturing CIV. This capability could be useful for modeling some ICC/EC plasmas.
- In RMF-driven FRCs friction between electrons and ions causes ion rotation. Excessive ion spin-up can cause  $n=2$  rotational instability, and the desired current would of course be reduced. In TCS and TCSU (as reported by A.M. Peters, C. Deards, etc.), drag due to some combination of neutral effects and ion viscosity evidently limits ion spin-up to acceptable levels. The plasma-neutral model in SEL/HiFi has been preliminarily applied to study the effect of neutral gas on azimuthal ion rotation.
- Finished the first stage of multi-block development for the HiFi/SEL code. This development allows for the computational domain to be composed of a set of blocks (logical cubes) connected in a structured fashion. This allows for much flexibility in the types of geometry that can be used for simulations, particularly non simply connected and non-axisymmetric geometries.
- An unstructured multi-block development is underway with the main data structures required in place. This development will allow for a unstructured collection of blocks, which will further increase the flexibility of the geometric possibilities for the computational domains in HiFi/SEL.
- Major progress has been made toward a scalable parallel solver, initially for the 2D SEL/HiFi code, but straightforwardly extendable to other 2D and 3D codes. The main effort during the Fourth Quarter of 2009 has been to develop accurate approximate Schur complements the application of physics-based preconditioning to more realistic problems. A new set of equations was developed for the full evaluation of the ideal MHD force

operator in arbitrary geometry and coordinate systems. This led to an understanding that a more accurate implementation requires the computation and use of second spatial derivatives of the magnetic vector potential. This was accomplished, and led to a great increase in accuracy, as reflected in a greatly reduced number of nonlinear Newton iterations to convergence. A further problem, which caused the code to crash after many time steps, was found to be attributable to too loose Newton tolerance and inadequate spatial resolution. With those problem corrected, physics-based preconditioning now works reliably for a 2D dissipative MHD FRC model. This will be tested in the near future with incorporation of radial compression and a full implementation of Braginskii transport. The next step after that is to test weak scaling up to a much larger number of parallel processors.

- The 3D equilibrium code is now working. It solves the zero beta equilibrium equation  $j = \lambda * B$  where  $\lambda$  is constant along field lines but can have arbitrary profiles across flux surfaces where surfaces exist. The code computes an artificial temperature function,  $T$ , by solving the parallel diffusion equation  $\text{div}(b * \text{grad}(T)) = 0$  with  $T = 1$  on the magnetic axis and  $T = 0$  on and outside the separatrix ( $b$  is the magnetic field direction). Solutions have perpendicular numerical diffusion but it is small enough to allow parallel diffusion to flatten  $T$  along the field line, while the boundary conditions maintain a perpendicular gradient. The separatrix is located by tracing field lines launched from every mesh point and tagging that point as being inside or outside if the field line enters an injector or not. The  $T$  function can be used as a flux surface coordinate since it is constant along fields lines and on magnetic surfaces where they exist. A  $\lambda$  profile may then be specified as any function of  $T$  and it will be constant along field lines too. Solutions have been computed using a 2- $\lambda$  profile which assumes 2 different constant values in the open and closed field regions and makes a smooth but rapid transition. This model has 2 free parameters: the difference between the 2  $\lambda$  values, which measures how far the equilibrium is from the Taylor state, and the ratio of toroidal flux to injector flux, which increases as helicity is increased. Below a flux ratio of about 1 there are no closed flux surfaces and the only solution is the Taylor state. As the flux ratio is increased, solutions become possible which differ from the Taylor state by increasing amounts. Solutions are being compared to magnetic probe measurements from the HIT-SI experiment. Work is underway make the code faster by adding multigrid preconditioning and upgrading the paralleliz

## Development of a Scalable Parallel Solver (*Alan Glasser*)

### Accomplishments

Major progress has been made toward a scalable parallel solver, initially for the 2D SEL/HiFi code, but straightforwardly extendable to other 2D and 3D codes. The main effort during the Fourth Quarter of 2009 has been to develop accurate approximate Schur complements the application of physics-based preconditioning to more realistic problems. A new set of equations was developed for the full evaluation of the ideal MHD force operator in arbitrary geometry and coordinate systems. This led to an understanding that a more accurate implementation requires the computation and use of second spatial derivatives of the magnetic vector potential. This was accomplished, and led to a great increase in accuracy, as reflected in a greatly reduced number of nonlinear Newton iterations to convergence. A further problem, which caused the code to crash after many time steps, was found to be attributable to too loose Newton tolerance and inadequate spatial resolution. With those problem corrected, physics-based preconditioning now works reliably for a 2D dissipative MHD FRC model. This will be tested in the near future with incorporation of radial compression and a full implementation of Braginskii transport. The next step after that is to test weak scaling up to a much larger number of parallel processors.

## Two-fluid and Transport Group (*C. R. Sovinec, E. D. Held, J.-Y. Ji, and J. B. O'Bryan*)

### Accomplishments

Over the quarter of funding ending on 12/31/09, the Two-fluid and Transport Group streamlined the fits used for collisional transport coefficients in plasma with varying magnetization and benchmarked NIMROD's implementation of the Braginskii version on sound and magneto-acoustic wave damping. We have also developed a method to solve the general moment equation to a specified order in the gyro-radius.

- We have finalized fitting formulas for electron transport coefficients at arbitrary magnetization to 1% accuracy. The formulas for the heat flow and friction are much simpler than the previous fits. We have also developed formulas for viscosity coefficients, where we find that the errors in Braginskii's coefficients are less significant (<7%) than those in heat flow and friction.
- Our implementation of Braginskii's magnetization effects for collisional heat flow in NIMROD has been verified on sound and magnetoacoustic waves. The problems are linear but are run as nonlinear computations with small-amplitude perturbations to exercise the coding for the nonlinear transport coefficients. In the plots shown in Figure 1, the background number density and magnetic field strength are varied in different computations to change the magnetization ( $\Omega\tau \sim BT^{3/2}/n$ ) while keeping the Alfvén speed and  $C_s \equiv \sqrt{\gamma(T_i + T_e)/m_i}$  constant. The sound wave is unaffected, but the perpendicular magnetoacoustic wave is influenced, as expected analytically. Parameters in both computations have been chosen to maximize damping of the two waves at low magnetization (see Figure 2) to make the tests sensitive. Results with the high magnetization limit of the Braginskii formulas are also shown in Figure 1 for comparison.
- In the small gyro-radius ordering, we have developed a systematic method of solving general moment equations. In the lowest order, we have found the general solution, which is a generalization of the CGL tensor to higher rank tensors. In the first and second

orders, we have simplified closure relations. The heat flow consists of the classical diamagnetic flow, integral form of parallel flows, and cross-field terms. The viscous stress consists of the parallel stress and terms driven by gradients of the flow and heat flow, and the divergence of the parallel third rank tensor moment.

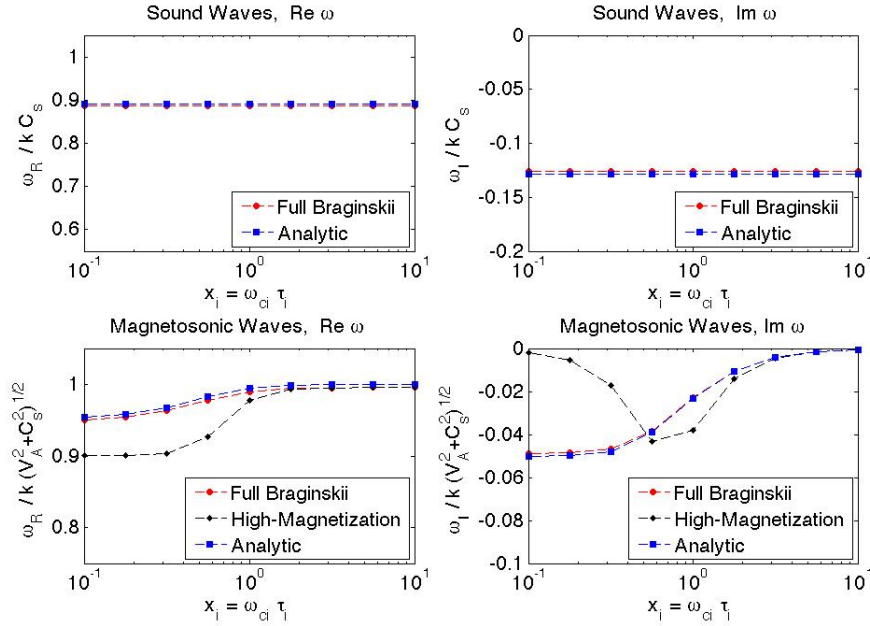


**Figure 1.** Verification tests of nonlinear thermal conductivity coefficients in the Braginskii model. As magnetization is varied, the sound wave (top) frequency and damping rate are unaffected, but the magnetoacoustic wave (bottom) transitions from high to low damping.

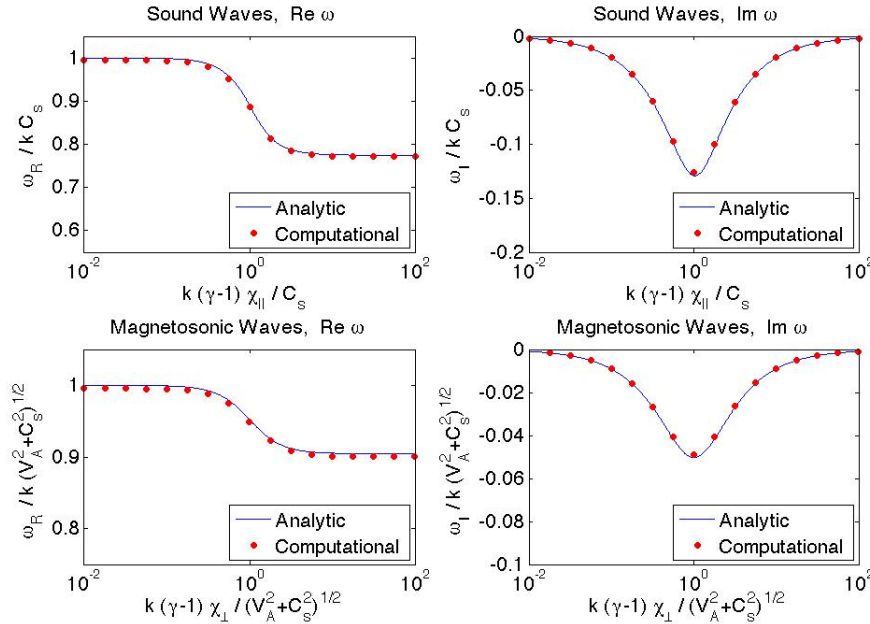


**Figure 2.** Frequency and damping rates of sound and magnetoacoustic waves as thermal conduction is varied.

## FLR and Kinetic Effects Group (*R. Milroy and C. Kim*)

We continue with NIMROD simulations of rotating magnetic fields (RMF) to form and sustain FRCs. We have begun working with the PIC model in NIMROD so that it can be used to evaluate the role of energetic ions in FRC stability.

### Accomplishments

- Progress continues with NIMROD simulations of rotating magnetic field (RMF) current drive for FRC formation and sustainment. Simulations were performed with an RMF time history designed to form an FRC, after which the RMF rapidly switched off. It was found that with even-parity antennas the field lines do not close after switching the RMF off. However, with odd-parity antennas the field lines do close and the FRC completely *heals* after the RMF is switched off. Post-processing torque analysis routines have been written to evaluate the main torques applied to the plasma in the RMF region. These include the torque transmitted from the RMF antennas to the plasma, viscous drag on the radial wall due to the induced plasma rotation, and the magnetic torque transmitted through the axial ends by the winding of the open magnetic field lines. This last torque can be thought of as an end-shortening effect. These are the main contributors to plasma spin-up and balance to within a few percent. We find that the back torque from twisting the open field lines is about 25 – 30 percent of the RMF torque and could be larger depending on the assumed resistivity boundary conditions. This will be refined when a new probe is inserted in the TCSU experiment so a comparison can be made. In most cases the RMF torque agrees well with an analytic expression that has been used for experimental analysis.
- NIMROD now has full orbit Lorentz PIC particle pushing in a rectangular grid FRC. Special routines have been added for a uniform regular mesh that greatly improves the PIC performance. Using these particles, we have performed some particle tracing simulations to understand the equilibrium orbits of ions in an FRC configuration with 4.15 mWb of trapped flux. The higher energy ions have very unique orbits that lie outside the usual MHD regimes. Figure 1 shows a sequence of particle orbits, with each sub-figure showing a single orbit over many transit times. The FRC flux is shown as a transparent green surface, and two sets of magnetic field lines are colored by their magnitude (one set approximately the last closed field line and the other set the first open field line). The particle orbit is colored by the toroidal velocity. By coloring the particles by their toroidal velocity the time evolution of the trajectory is obscured. However, another interpretation of the plot is to view the particles as a closed trajectory of a phase space plot in  $(x, y, z, v_\theta)$ . Figure 1a shows a betatron orbit with an  $m=2$  structure, while Fig. 1b shows a different view of the same particle orbit. This particular betatron orbit exhibits an  $m=2$  lobe structure that shifts 90 degree as the orbit crosses the symmetry plane. Betatron orbits with larger "m-mode" have also been observed. Another example is the resonant orbit (Fig. 1c). Note that the toroidal velocity is always positive. This is typical for most of the energetic population. For comparison, Fig. 1d shows a low energy orbit. The usual gyro-orbit is clear in the tight spirals. Also present but not quite as obvious is the drift motion of gyrocenter due to curvature and gradients in magnetic field. Beyond single particle traces we can also look at the equilibrium distribution function. We initialize the particle sample (millions of particles) as an isotropic Maxwellian. We push the particles many transit times until the distribution reaches a steady state.

Observation of the velocity space distribution shows a strong anisotropy in the  $v_\theta$  direction, with particles strongly preferring the co-rotating direction. This anisotropy is more pronounced as the temperature is increased. The velocity space distribution plots are shown in Fig. 2. Figures 2a and 2c show the initial isotropic loading for 100eV, and 2.5KeV respectively. The resulting steady state distribution of particles after many transit times is shown in Figures 2b and 2d. For the 100eV case, the distribution (plotted in  $(v_\theta, |v_z|)$ ) remains relatively symmetric. For the 2.5KeV case, the distribution evolves to a strongly co-rotating one.

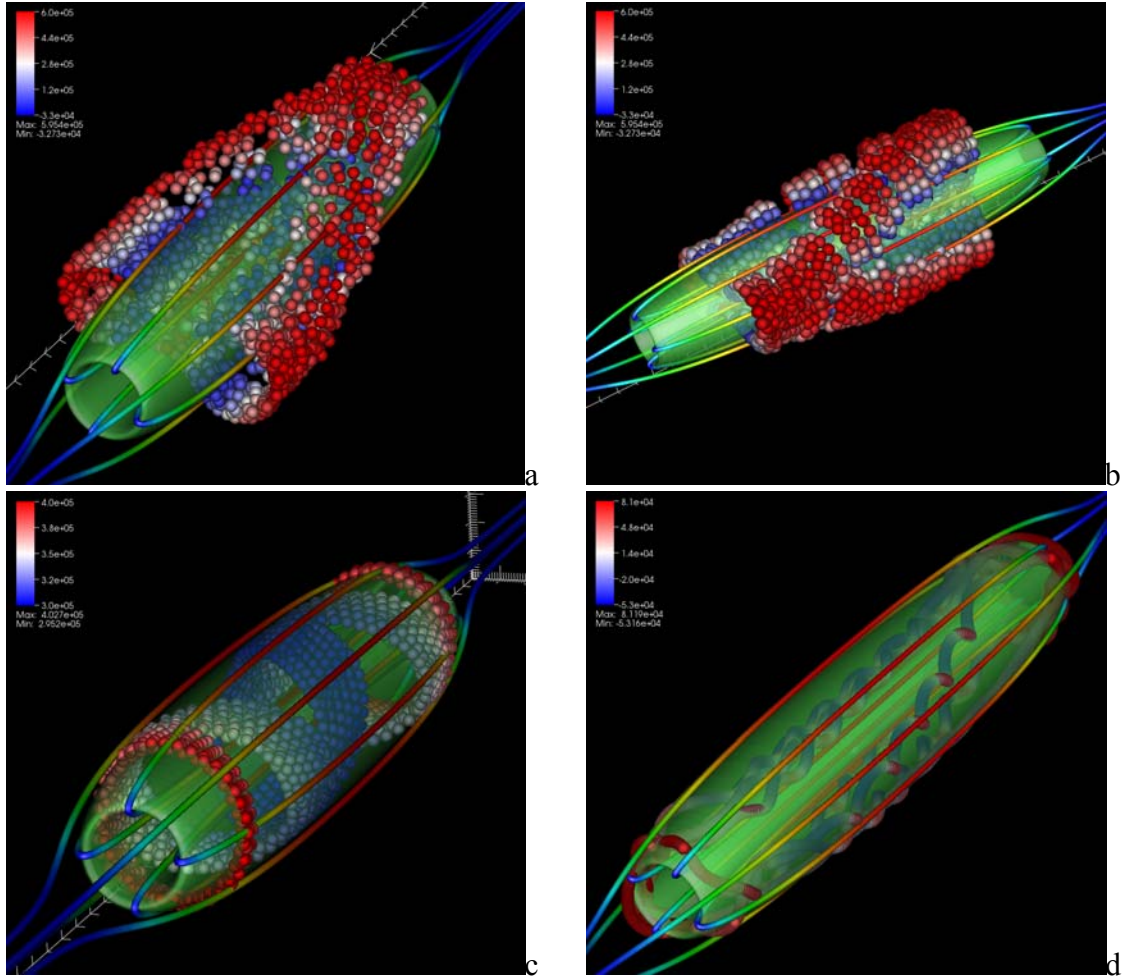
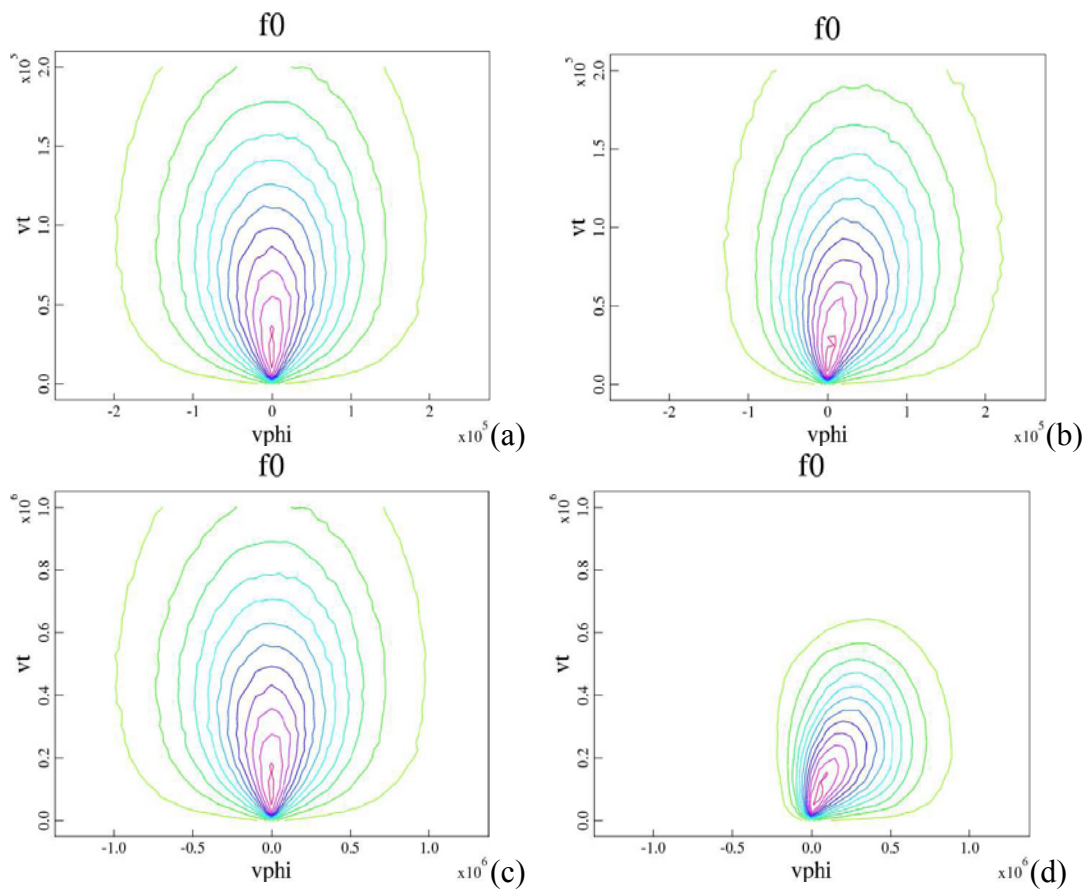


Fig. 1 Particle orbits for a single particle in an FRC field.



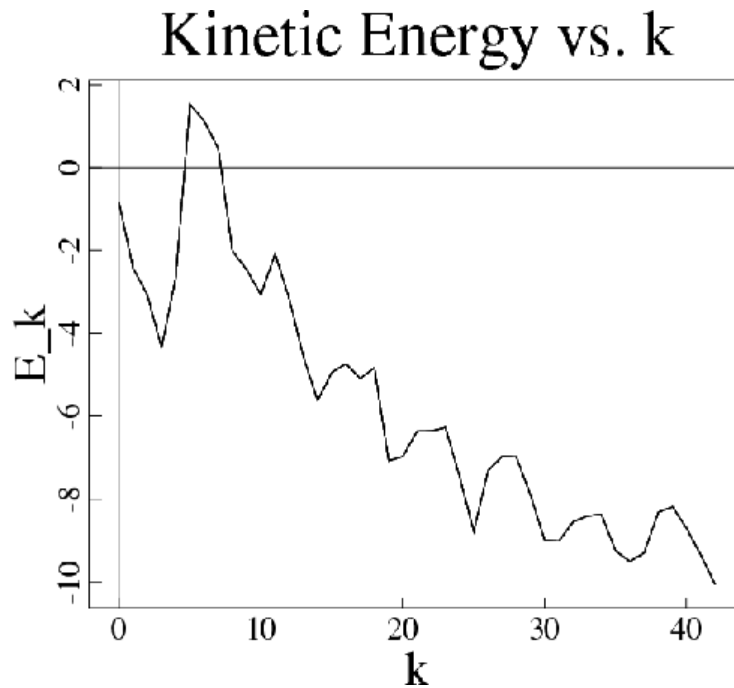
**Fig2 Velocity space distribution plots. Initial (a) and final (b) velocity distributions for a 100 eV ion. Initial (c) and final (d) velocity distributions for a 2.5 keV ion.**

## Interfacing Group (*B. A. Nelson, C. C. Kim, S. D. Griffith*)

The IG is tasked with assisting in computational support for the twelve collaborating ICC experiments (along with the three physics groups).

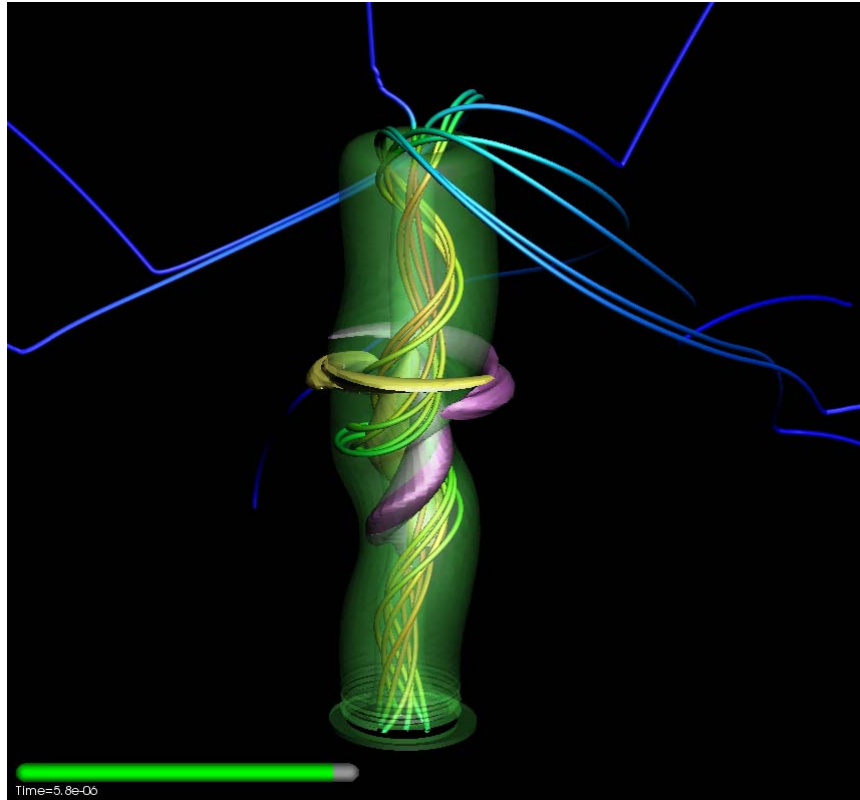
### Accomplishments:

- Continue working with MST on NIMROD simulations. Computed the first toroidal linear simulations of MST. Results of edge tearing mode simulation show good agreement with experimental measurements on MST. These results have been included in an article submitted for review (C. K. Kim, second author).



Spectrum of LDX kinetic energy vs. toroidal mode number.

- Breakthrough with the LDX NIMROD simulations, working with Dr. Jay Kesner of M.I.T.: At 43 modes ( $n=0-42$ ) the spectrum finally converges (plot shows kinetic energy vs. mode number). At sufficient toroidal resolution, the growth rate no longer peaks at the highest  $n$  mode as was observed (and distressing) in simulations with few modes. The plot of mode energy shows a strong peak at  $n=5$  with higher harmonics very prominent at higher  $n$ . Lesson learned in necessity of resolving the toroidal direction.
- Breakthrough in NIMROD coplanar gun (Caltech-like) driven kink simulations: Finally formed a free boundary kink. Looks like the key control parameter was allowing the density to drop sufficiently in the columnation region. Further studies are planned.



**Caltech-like NIMROD simulations of free-boundary kink: Green is the total  $B_\phi$ , magnetic field lines colored by magnitude, and the  $n=1$  VR perturbation in purple and yellow. At 5.8 microseconds into the simulation.**

- The IG presented an overview of PSI-Center simulation results at the APS meeting, including a poster and talk at the PSI-Center Collaborators Session.
- Received ARRA funds to improve local cluster capabilities, communications, and visualization:
  - Will increase number of processors on local cluster from 192 to 256, add more memory per processor, and a larger RAID drive for archiving.
  - Univ Wisc and Utah State groups will each purchase 2 8-way machines for local computing.
  - New visualization computer, including large hires screen and 3D capabilities, upgraded LCD projector, and telecommunications equipment.